Journal of Cell Science 111, 413-423 (1998)
Printed in Great Britain © The Company of Biologists Limited 1998
JCS7173

Changes in protein composition of meiotic nodules during mammalian meiosis

Annemieke W. Plug[1], Antoine H. F. M. Peters[2], Kathleen S. Keegan[3], Merl F. Hoekstra[3], Peter de Boer[2] and Terry Ashley[1]

[1]Department of Genetics, Yale University School of Medicine, New Haven, CT 06510, USA
[2]Wageningen Institute of Animal Sciences, Wageningen Agricultural University, Wageningen, Netherlands
[3]ICOS Corporation, Bothell, Washington 98021, USA
*Author for correspondence (e-mail: terry.ashley@qm.yale.edu)

Accepted 9 December 1997: published on WWW 27 January 1998

SUMMARY

Homologous chromosome synapsis and meiotic recombination are facilitated by several meiosis-specific structures: the synaptonemal complex (SC), and two types of meiotic nodules: (1) early meiotic nodules (MNs), also called zygotene nodules or early recombination nodules, and (2) late recombination nodules (RNs). The former are thought to be nucleoprotein complexes involved in the check for homology preceding, or accompanying synapsis, while the latter have been shown to be involved in reciprocal recombination. We have examined by immunocytochemistry the meiotic localization of a series of proteins at sites along the asynapsed axial elements prior to homologous synapsis and at sites along the SCs following synapsis. Several of the proteins examined have been implicated in repair/recombination and include RAD51, a mammalian homolog of the *Escherichia coli* RecA protein; Replication Protein-A (RPA), a single-strand DNA binding protein; and MLH1, a mismatch repair protein which is a homolog of the *E. coli* MutL protein. In addition two proteins were examined that have been implicated in meiotic checkpoints: ATM, the protein mutated in the human disease Ataxia Telangiectasia, and ATR, another member of the same family of PIK kinases. We present evidence that these proteins are all components of meiotic nodules and document changes in protein composition of these structures during zygonema and pachynema of meiotic prophase in mouse spermatocytes. These studies support the supposition that a subset of MNs are converted into RNs. However, our data also demonstrate changes in protein composition within the context of early MNs, suggesting a differentiation of these nodules during the process of synapsis. The same changes in protein composition occurred on both the normal X axis, which has no homologous pairing partner in spermatocytes, and on the axes of aberrant chromosomes that nonhomologously synapse during synaptic adjustment. These findings suggest that DNA sequences associated with MNs still must undergo an obligatory processing, even in the absence of interactions between homologous chromosomes.

Key words: Meiotic nodule, Meiotic synapsis, Meiotic recombination, RAD51, RPA, MLH1, ATM, ATR

INTRODUCTION

The meiotic segregation of a complete set of chromosomes into each haploid nucleus requires several meiosis-specific structures that facilitate synapsis and recombination between homologous chromosomes. These structures include the synaptonemal complex (SC) and two types of 'meiotic nodules'. The SC is a tripartite structure consisting of two axial/lateral elements and a central element (Moses, 1968). Following premeiotic DNA replication, the chromosomes start to condense and axial elements begin to form between sister chromatids. The chromatin itself is organized into loops with only the chromatin at the base of the loops attached to the axial element (Weith and Traut, 1980). When the autosomes synapse in zygonema, the axial elements of homologous chromosomes align and are united by a central element and transverse filaments to form the synaptonemal complex. Once synapsed, the axial elements are called lateral elements (Moses, 1968; Wettstein et al., 1984).

In electron microscopic studies of meiotic cells, two different types of 'nodules' are found associated with the axial elements or with partially or fully formed SCs: (1) variously sized nodules (30-200 nm) found on unsynapsed axial elements and newly formed SCs in zygonema and early pachynema, and (2) more uniform nodules (100 nm in their longest dimension) found on SCs in mid-late pachynema. The former have been referred to as meiotic nodules (Anderson and Stack, 1988), zygotene nodules (Albini and Jones, 1987), or early recombination nodules (Carpenter, 1987) and are thought to be involved in the check for homology that precedes or accompanies synapsis (Albini and Jones, 1987; Anderson and Stack, 1988; Carpenter, 1987). Since the mechanism of the

check for homology is unknown and these structures are present during leptonema, zygonema and early pachynema, we prefer the less biased term meiotic nodule (MN). The latter type of nodule is associated with SCs in mid-pachynema and are referred to as recombination nodules (RNs) in reference to their presumed involvement in reciprocal recombination (Carpenter, 1979). Although both types of nodules have long been assumed to be nucleoprotein complexes, identification of specific protein components had to await the application of antibody technology to meiotic preparations.

Such immunolocalization techniques are now available, however, certain criteria must be met before a protein can be considered a component of a meiotic nodule. The most rigorous proof is direct immunogold localization of an antibody against the protein to an identifiable meiotic nodule on an electron micrograph. Once one protein has been positively identified in this manner, by inference other proteins that colocalize with it by fluorescence immunocytochemistry can be considered components. However, other criteria can also constitute strong circumstantial evidence. If the protein appears in the same places and under the same set of circumstances as have been reported for meiotic nodules or recombination nodules, that protein is likely to be a component of that type of nodule.

Based on their demonstrated molecular biochemical properties, certain proteins are prime candidates for participatory components of one or both type of nodules. The *E. coli* protein RecA is the prototype molecule capable of facilitating a DNA-specific homology search by catalyzing homologous DNA pairing and strand exchange essential for repair and recombination. Studies on early events in meiotic prophase have therefore focused on eukaryotic homologs of RecA resulting in the identification of several such homologs which have subsequently been shown to be associated with synapsing chromosomes during early meiotic prophase. These include Dmc1 and Rad51 in yeast (Bishop, 1994; Rockmill et al., 1995); Lim15 and Rad51 in plants (Terasawa et al., 1995) and RAD51 in mouse (Ashley et al., 1995; Plug et al., 1996). Each of these studies proposed that the identified RecA homologues were components of early meiotic nodules, but definitive proof was lacking. More recently, however, Anderson et al. (1997) used immunogold labeling to conclusively demonstrate that an antibody which recognizes plant RAD51 and LIM15 localizes to early meiotic nodules (MNs) in lily meiocytes providing the requisite anchor-point mentioned above for further MN colocalization.

MLH1 is a mismatch repair protein involved in mammalian meiosis (Baker et al., 1996; Edelmann et al., 1996). The number and distribution of MLH1 foci in mouse spermatocytes corresponds to the reported number and distribution of chiasmata (Polani and Jagiello, 1976). These are the same criteria that were used to argue that recombination nodules (RNs), seen along the SC during mid pachynema are involved in reciprocal recombination (Carpenter, 1975). Ergo, MLH1 can be considered a component of RNs and used as a reference protein for RN colocalization studies. Male mice deficient for the MLH1 protein do not form chiasmata and arrest in meiotic metaphase I, providing additional evidence that MLH1 is essential for reciprocal recombination (Baker et al., 1996).

By using RAD51 and MLH1 as reference proteins for MNs and RNs respectively, we have studied the meiotic localization of a number of other proteins. RAD51-mediated strand exchange is inefficient in the absence of some other single-strand (ss) DNA binding proteins (Baumann et al., 1996; Sung, 1994). The best characterized eukaryotic single-strand binding protein is replication protein A (RPA), a trimeric complex composed of 70, 32 and 14 kDa subunits (Fairman and Stillman, 1988; Wold and Kelly, 1988). The 70 kDa subunit binds directly to ssDNA where it plays a role in DNA replication, nucleotide excision repair and genetic recombination (Coverley et al., 1991, 1992; Fairman and Stillman, 1988; Heyer et al., 1990; Moore et al., 1991; Wobbe et al., 1987; Wold and Kelly, 1988). The localization studies presented below suggest that RPA is a component of both MNs and RNs.

Since meiotic synapsis and recombination can be expected to involve lesions in the DNA, it is not surprising that several mitotic checkpoint proteins are also present in meiotic nuclei. Two such mammalian checkpoint proteins, ATR and ATM, are structurally related members of a family of phosphatidylinositol 3-kinase (PIK)-like kinases (Hoekstra, 1997; Savitsky et al., 1996). Keegan et al. (1996) showed that ATR localizes to sites along asynapsed axial elements during zygonema and pachynema, while ATM localizes to sites along synapsed SCs suggesting that these proteins might be components of early meiotic nodules. The current study demonstrates that both of these proteins colocalize with RAD51 at sites on asynapsed and synapsed axes, respectively, confirming the contention that they are components of MNs.

Our observations not only confirm that RAD51, RPA, ATR and ATM are components of MNs, but support the assumption that a subset of MNs are converted into RNs by undergoing a change in protein composition. However, our data also demonstrate a change in protein-components within the context of MNs, suggesting a differentiation in early MNs associated with axial elements preceding synapsis, and MNs associated with the synaptonemal complex. Although delayed, similar changes in protein composition occur in MNs on the asynapsed X axis, that has no homolog in spermatocytes, and on nonhomologously synapsing autosomal axes in translocation double heterozygotes. These sequential changes suggest that RAD51-associated DNA sequences must undergo an obligatory processing that is not dependent on interhomolog interactions.

MATERIALS AND METHODS

Meiotic preparations

Surface spreads were prepared from spermatocytes of 15- to 21-day-old male (C57-Bl/6) mice using a ‘dry down’ technique (Peters et al., 1997b). All slides are evaluated under ×40 phase microscopy as soon as they are made and only slides with well-spread nuclei and minimal nucleoplasmic background are selected for antibody labeling.

Antibodies

All antibodies used in the current study had been used in previously published cytochemical studies where their specificity was demonstrated. A polyclonal mouse antiserum to the Syrian hamster COR1 protein, a component of the axial/lateral elements, was used to visualize the axial elements and the synaptonemal complexes in the meiotic preparations (Dobson et al., 1994). The COR1 protein is

equivalent to the SCP3 protein isolated from rat spermatocytes (Lammers et al., 1994).

Rabbit polyclonal anti-human RAD51 antibody, which recognizes both mouse RAD51 and DMC1, was generated by immunization with purified recombinant human RAD51 protein (Haaf et al., 1995), and affinity purified. Control experiments in which the anti-human RAD51 serum was preincubated with the recombinant human RAD51 protein resulted in no staining; while preincubation with mammalian DMC1 protein resulted in a focal pattern indistinguishable from the RAD51 antibody staining, thereby demonstrating the specificity of the focal RAD51 pattern observed in meiotic preparations.

Polyclonal RPA serum was raised in rabbit using purified recombinant human RPA (He et al., 1995). In addition, a monoclonal antibody specific for the 70 kDa subunit of the human RPA protein was used (Kenny et al., 1990). The monoclonal antibody against the human MLH1 protein (clone G168-15.3) was obtained from Pharmingen. Localization of MLH1 in meiotic prophase I has been described previously (Baker et al., 1996).

The ATR monoclonal antibody, 224C, was generated by injection of an ATR-Gst fusion protein expressing amino acids 2,341-2,644 of ATR (antigen DH-2, see Keegan et al., 1996).

Since all the antibodies used in these studies were raised in rabbits or mice, and since use of secondary antibodies with attached fluors requires species recognition, triple labeling with RAD51, RPA and COR1 or with RPA (or RAD51), MLH1 and COR1 was not done.

Antibody detection and computer analysis

Antibody incubation and detection procedures were as described previously (Ashley et al., 1995). Goat anti-mouse IgG-rhodamine-conjugated and goat anti-rabbit IgG-FITC-conjugated (Pierce) secondary antibodies were used for detection. All preparations were counterstained with 4′,6′ diamino-2-phenylindole (DAPI, Sigma) and mounted in a DABCO (Sigma) antifade solution. The preparations were examined on a Zeiss Axioskop (×63 and ×100, 1.2 Plan Neofluor oil-immersion objective). Each fluorochrome (FITC, rhodamine and DAPI) image was captured separately as an 8-bit source image using a computer assisted cooled CCD camera (Photometrics CH 220). Before merging, each image was enhanced to reduce background noise uniformly over the entire image using Adobe Photoshop (‘Levels’ setting). Since the merge function of ‘Gene-Join, Max-Pix’ (custom software developed by Tim Rand, see Ried et al., 1992) evaluates and registers only the more intense pixel of each image, the relative intensity of each image was adjusted to allow the dimmer RAD51 and MLH1 signals to be detected against the brighter COR1 signal. In a separate study (L. K. Anderson and T. Ashley, unpublished observations), the background staining for MLH1 was determined by counting any focus (fluorescent spot) over the DAPI, but not the SC image. These ‘background’ spots were generally less intense and smaller than those over the SCs and ranged from 3 to 42 per nucleus. The average number of foci per square micrometer was 0.53 for SCs vs 0.018 for background (n=26). No relationship between the number of foci and background was found (r^2=0.04, n=14). Merges of the colocalization of foci (RAD51 and ATR; RAD51 and RPA) were done in Adobe Photoshop (layers).

T(1;13)70H/T(1;13)1Wa double heterozygous translocation

Spermatocytes of four 3- to 4-week-old mice heterozygous for the T(1;13)70H and T(1;13)1Wa translocations were spread using a dry-down technique (Peters et al., 1997b). Juvenile males were used to enhance the percentage of zygotene and early pachytene spermatocytes available for study. Offspring were generated by crossing homozygous T(1;13)70H females with homozygous T(1;13)1Wa males. Both translocations are carried in a Swiss random bred stock. Surface spread spermatocytes of the T70H/T1Wa double heterozygous translocation mice were incubated with a polyclonal antibody against RAD51 or RPA (both raised in rabbit), in combination with an antibody against COR1, a component of the lateral element (raised in mouse).

RESULTS

Temporal staging of meiotic prophase

As discussed above, nodular structures are found on the axial elements prior to synapsis, or associated with the SC after synapsis. A means of identifying the axial elements is therefore key to following the progression of nodular development. The COR1 protein is a component of the axial/lateral elements of the synaptonemal complex (Dobson et al., 1994). Staining with antibodies against COR1 allows us to determine substages of meiotic prophase by following the formation and synapsis of the axial elements. Axial element formation begins in leptonema prior to homologous autosomal synapsis which occurs during zygonema. In spermatocytes, the zygotene stage takes approximately 1 day. Completion of synapsis of the autosomal homologs marks the transition to pachynema, a stage which lasts about 6 days in spermatocytes (Goetz et al., 1984; Oakberg, 1957). Pachynema can be divided into substages based on cytological criteria, the most characteristic of which is the synaptic behavior of the sex chromosomes (Moses, 1980). In early pachynema, synapsis between the X and Y chromosomes is not confined to the pseudoautosomal region, but includes extensive non-homologous synapsis (up to 90% of the Y). Once the X and Y have reached maximal synapsis, the heterologously synapsed region starts to desynapse and the X and Y axes begin to shorten and thicken. In mid pachynema, 10-35% of the length of the Y-axis remains synapsed with the X, but by the mid-late pachytene stage Y synapsis is reduced to less than 10%. Late pachynema is marked by an end-to-end association of the XY, a prominent sex body, and an axial thickening at both ends of the synaptonemal complex of autosomal bivalents. The correspondence between staging by heavy-metal staining and electron microscopy vs fluorescence labeling of an axial element component and fluorescence light microscopy has been verified (Ashley and Plug, 1998).

Spatial and temporal distribution of ATR relative to RAD51

Localization studies with affinity purified RAD51 and COR1 show that RAD51 is present on both the axial elements in leptonema-zygonema, and the synapsed SCs in early pachynema (data not shown). Keegan et al. (1996) found that the distribution of ATR, a DNA damage checkpoint protein, is similar to the pattern of RAD51 on asynapsed axes of zygotene spermatocytes. However, unlike RAD51, ATR is not found on synapsed axes. Here, double-labeling experiments with an affinity purified rabbit polyclonal serum against RAD51 (Fig. 1A) and a monoclonal antibody against ATR (Fig. 1B) demonstrate that ATR foci colocalize with a subset of RAD51 foci in zygotene nuclei, but not all RAD51 foci colocalize with ATR (Fig. 1C) in zygotene nuclei (Fig. 1D). Based on the differences in ATR vs RAD51 localization on asynapsed vs asynapsed plus synapsed axes, it seems likely that colocalization is confined to sites on the asynapsed axial elements. Colocalization of RAD51 and ATR is very transient during normal autosomal synapsis. However, if there is a delay

in completion of synapsis, the ATR localization is no longer restricted to foci, but begins to accumulate and coat the entire axes. This is not the case with RAD51, which remains focal in nature at discrete sites along the asynapsed axes.

Spatial and temporal distribution of RPA relative to RAD51

RPA first appears in a focal pattern along the SCs of synapsing meiotic chromosomes (Plug et al., 1997). To compare the temporal and spatial distribution of RAD51 and RPA on synapsed meiotic chromosomes, we reexamined the temporal localization of RAD51 foci in zygotene and pachytene spermatocytes. Fig. 2A shows a late zygotene nucleus in which some of the bivalents have already completed synapsis, while other bivalents are in the process of synapsis and one pair of homologs remain completely asynaptic. RAD51 foci are associated with the unsynapsed axial elements of the univalents and pairing forks, as well as the X-chromosome. RAD51 foci are also present along most of the SCs, however, some of the bivalents that have completed synapsis appear to have already lost all, or most, of the RAD51 foci. These observations suggest that the RAD51 foci begin to disappear from the SCs shortly after completion of synapsis. Fig. 2B shows a similar late zygotene nucleus, with some bivalents that have completed synapsis, others with pairing forks and another (the X) present as a univalent. In this nucleus RPA foci are found along the SCs, but not the unsynapsed axial elements.

Since some RAD51 foci remain transiently on synapsed axes, RAD51 and RPA foci associated with the autosomal bivalents in pachytene spermatocytes were counted (Table 1). In early pachynema an average of 66 (±15.2; *n*=21) RAD51 foci are associated with the autosomal SCs, compared to 136 RPA foci. Between early and mid pachynema the number of RAD51 foci drops by half (35.3±13.3, *n*=30), while the average number of RPA foci at this stage (120.3±18.4, *n*=20) remains close to the number found in early pachynema. Moreover, the coefficient of variation during this substage is much higher for RAD51 than for RPA (37 vs 15), supporting the impression of greater variability in number of RAD51 foci. The remaining RAD51 foci associated with the autosomal bivalents had almost disappeared by the transition to late pachynema. Since we used prepubertal mice (15-16 days old), the first wave of spermatogenesis had not yet completed the late pachytene stage which lasts about 4 days (Goetz et al., 1984). However, some spermatocytes from these mice have reached the transition to this stage and still have a small number of RAD51 foci (5±4, *n*=20)

Table 1. Number of foci associated with the synaptonemal complexes of the autosomes in pachytene spermatocytes

Pachynema substage	RAD51	RPA
Early	66.0±15.17 (*n*=21)	136.7±10.59 (*n*=20)
Mid	35.3±13.30 (*n*=30)	120.3±18.14 (*n*=20)
Mid-late	27.4±16.63 (*n*=25)	46.1±27.16 (*n*=27)
Late	4.8±4.0 (*n*=20)	2.5±3.85 (*n*=22)

Comparison of the number of RAD51 and RPA foci associated with the autosomal synaptonemal complexes in early-, mid-, and late-pachytene spermatocytes.

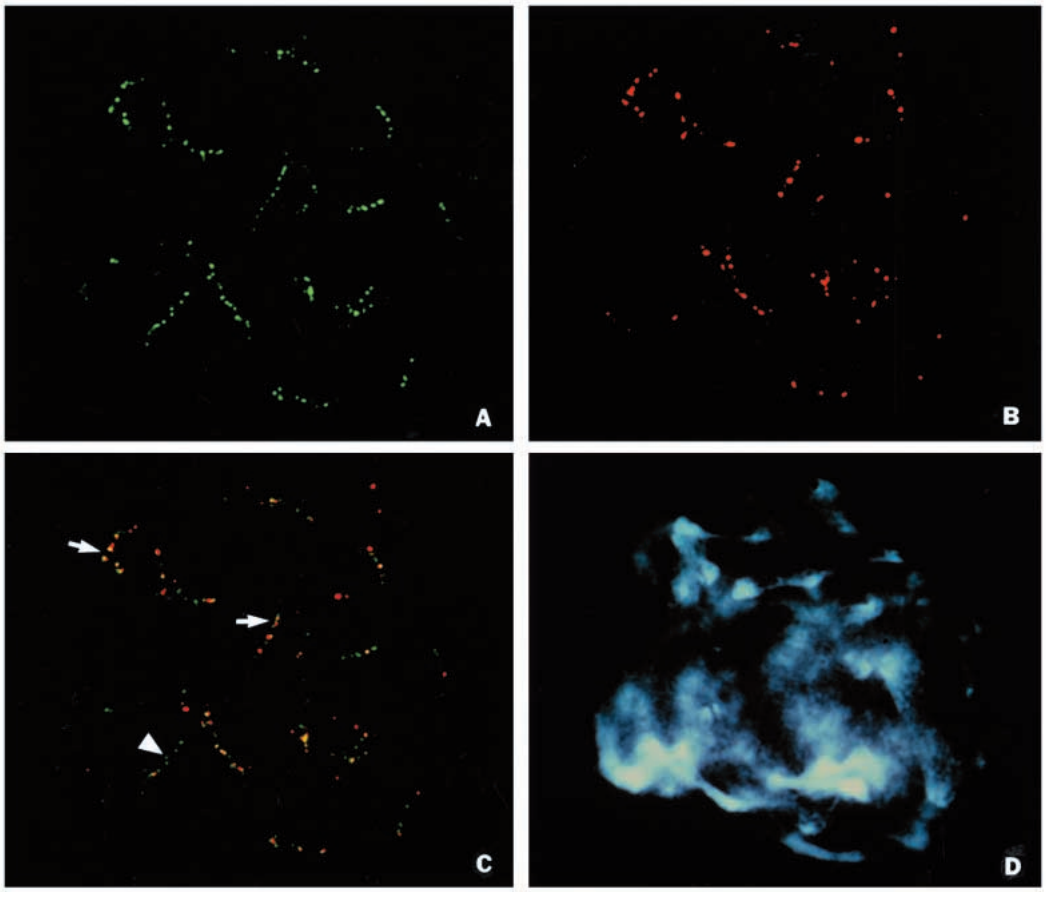

Fig. 1. Comparison of the spatial distribution of RAD51 and ATR (RAD51: green; ATR: red). (A) RAD51, (B) ATR, (C) RAD51 and ATR, and (D) DAPI, all show the same zygotene spermatocyte. The merged RAD51 and ATR image (C) shows that ATR colocalizes with some (yellow foci, arrow), but not all (green, large arrowhead), RAD51 foci. The green arrays of RAD51 foci probably represent asynapsed axes; yellow arrays, synapsed sites.

present along the autosomal SCs. Observations on preparations from mature animals show that the remaining RAD51 foci completely disappear during late pachynema (data not shown).

To study in more detail the temporal and spatial distribution of RPA relative to RAD51, we performed double-labeling experiments with a rabbit polyclonal antibody against RAD51 and a mouse monoclonal antibody for the 70 kDa subunit of RPA (Fig. 2C,D). The localization pattern is consistent with the RAD51/COR1 and RPA/COR1 results. In zygotene nuclei, some RAD51 (only) foci are present in linear arrays (presumptive univalents, or unsynapsed axes); some arrays of RAD51 and RPA foci colocalize (presumptive newly synapsed axes). The RPA (only) foci are presumed to be sites on synapsed axes where RAD51 is no longer present.

Spatial and temporal distribution of ATM relative to RPA

ATM localizes to sites along synapsed axes (Keegan et al., 1996) and colocalizes at these sites with RPA (Plug et al., 1997). The temporal appearance and disappearance of these proteins also coincides (Plug et al., 1997).

Spatial and temporal distribution of RAD51 and RPA relative to MLH1

MLH1, a DNA mismatch repair protein, localizes to sites of reciprocal recombination on meiotic chromosomes, suggesting that MLH1 is a component of RNs (Baker et al., 1996). In spermatocytes MLH1 foci begin to appear in early pachynema and reach an average number of 1.17 MLH1 foci per autosomal bivalent, or an average of 22 autosomal foci/nucleus, in early-mid pachynema (Baker et al., 1996). In order to determine whether MLH1 foci colocalize with RAD51 or RPA, we performed double-labeling experiments using a mouse monoclonal antibody for MLH1 and rabbit polyclonal antiserum against RAD51 or RPA. Fig. 3B shows a spermatocyte in early-mid pachynema double-labeled with RAD51 and MLH1. With the exception of

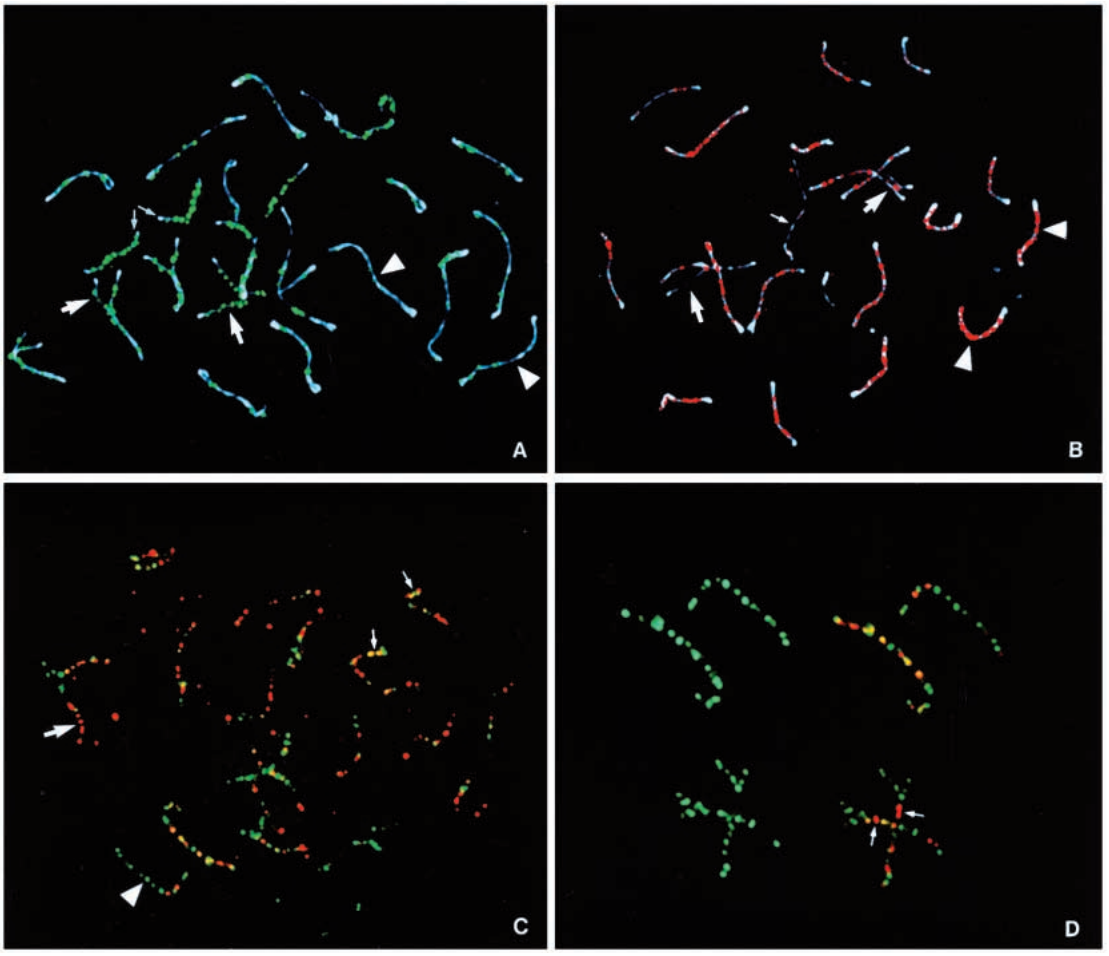

Fig. 2. Comparison of the temporal and spatial distribution of RAD51 and RPA (COR1: white; RAD51: green; RPA: red). (A) Zygotene spermatocyte: RAD51 foci are associated with the unsynapsed axial elements of pairing forks (arrows) and univalents (small arrows), but have disappeared from some of the synapsed SCs (arrowheads). (The blueish appearance of some of the axial elements is an artifact of photographing the image from the computer screen.) (B) Zygotene spermatocyte: RPA foci are present along the SCs (arrowheads), but not the unsynapsed axes of pairing forks (arrow). (C and D) Double-labeling for RAD51 (red) and RPA (green). (C) A zygotene nucleus stained for both RAD51 and RPA. Green arrays of foci are interpreted as RAD51 foci associated with unsynapsed axial elements or bivalents that have just completed synapsis (arrowheads), while red RPA foci indicate sites where synapsis has already occurred or is in progress (arrows). Yellow foci mark sites were RAD51 and RPA colocalize (small arrows). (D) The localization of RAD51 foci in relation to RPA foci shown in more detail. Following synapsis, both RAD51 and RPA foci are present along the SCs, with several foci colocalizing (Fig. 2D, yellow foci). Since RAD51 remains associated with the synapsed bivalents only briefly, many synapsed sites have only RPA foci (red, arrows).

Table 2. Comparison of the number of MLH1 foci colocalizing with RAD51 vs the number of MLH1 foci colocalizing with RPA in mid-pachytene spermatocytes

Number of foci in mid-pachynema		MLH1 foci colocalizing with RAD51 or RPA	
RAD51	MLH1		
43.1±7.9	21.4±2.4	2.5±1.2	(12%; *n*=9)
RPA	MLH1		
110±7.0	21.4±1.3	20.6±2.0	(96%; *n*=9)

the MLH1 focus at the base of the XY bivalent, only one of the MLH1 foci colocalize with RAD51. In contrast, Fig. 3D shows a spermatocyte at a similar stage labeled with antibodies against RPA and MLH1. Many of these MLH1 foci colocalize with RPA foci. The quantitation of these double-labeling experiments is summarized in Table 2. Spermatocytes in mid pachynema were selected based on the number of RAD51 or RPA foci. As described above, the average number of RPA foci at this stage is around 120, while the number of RAD51 foci in this subset varies from 30 to 50. Only about 12% of the MLH1 foci colocalize with RAD51 in mid pachytene spermatocytes, while at the same substage more then 96% of the MLH1 foci colocalize with RPA.

Spatial and temporal distribution of RAD51 and RPA during asynapsis and non-homologous synapsis

During normal synapsis, RAD51 foci associated with the axial elements disappear shortly after formation of the synaptonemal complex. However, the X-chromosome has no homologous partner in spermatocytes and consequently can never completely synapse. RAD51 foci remain associated with the asynapsed X-axis during early and mid-pachynema (Fig. 4A). As is the case with asynapsed autosomal axes, RPA foci are not found on the axial element of the X in early to mid-pachynema (Fig. 4B). However, despite the continued asynapsed state of the X, RPA foci appear along the X axis by mid- or mid-late pachynema (Fig. 4C). The appearance of RPA along the X axial element coincides with the time of disappearance of the RAD51 from similar focal sites (Fig. 4D). By the transition to late pachynema, neither RAD51 nor RPA foci are any longer found along the X-axis.

To study the temporal and spatial distribution of RAD51 and RPA during nonhomologous synapsis, we examined a chromosome aberration (a double translocation heterozygote involving chromosomes 1 and 13) in which normal progression of synapsis is disturbed. Fig. 5A shows the homologs for both chromosome 1 and 13 and indicates the T70H and T1Wa breakpoints. The double translocation results in two pairs of largely homologous translocation chromosomes, however, the homologous chromosome 1 regions between the T70H and T1Wa breakpoints are now present on non-homologous translocation chromosomes. During meiotic chromosome synapsis, the translocation chromosomes form heteromorphic bivalents which are characterized by an unsynapsed axial loop,

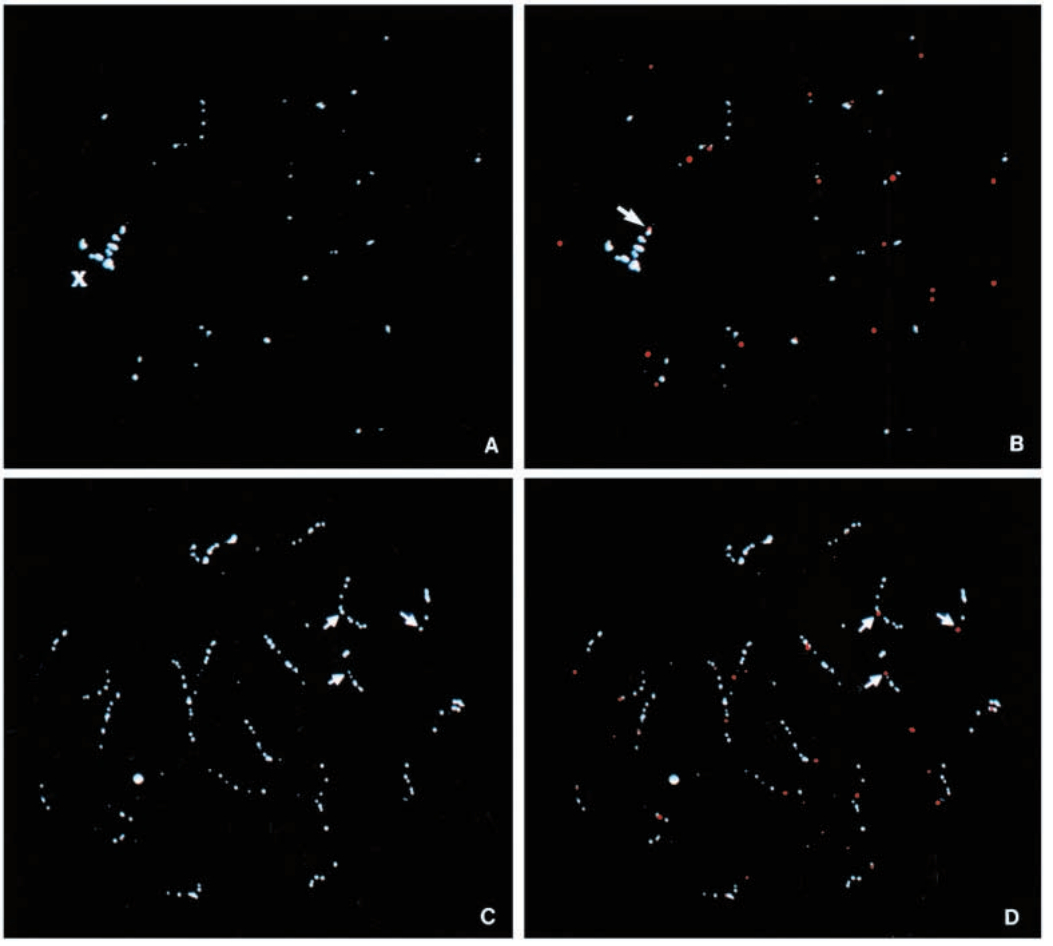

Fig. 3. Comparison of the spatial distribution of MLH1 and RAD51, and MLH1 and RPA (RAD51, RPA: white; MLH1: red). (A) Mid pachytene spermatocyte showing RAD51 distribution. The X chromosome can be identified by the concentration of RAD51 foci along its asynapsed axis. (B) Same nucleus showing both RAD51 and MLH1. Colocalization of MLH1 and RAD51 at the distal end of the X is indicated by an arrow: On the autosomes RAD51 and MLH1 sporadically colocalize. (C) Mid pachytene spermatocyte showing RPA signals. (D) Same nucleus showing both RPA and MLH1 signals: all MLH1 foci colocalize with RPA foci. Examples are indicated by arrows. One intense red spot and several additional red spots of very low intensity are not associated with linear arrays of RPA and probably represent background.

representing the nonhomologous portions of translocated chromosome 1 regions (Fig. 5B).

Resolution of the unsynapsed axial loops of the translocation chromosomes may occur by either of two types of non-homologous synapsis (de Boer et al., 1986; Peters et al., 1997a): heterosynapsis concurrent with homologous synapsis during zygonema (Ashley, 1988; Ashley and Russel, 1986), or delayed heterosynapsis in mid- to late-pachynema by a process termed synaptic adjustment (Moses and Poorman, 1981). The localization of RAD51 and RPA differ during the process of synaptic adjustment of the unsynapsed axial loop of the 13^1 translocation bivalent. RAD51 foci are associated with the asynapsed axial element of the 13^1 loop (Fig. 6A,C). When synaptic adjustment occurs, RAD51 foci remain on the newly synapsed SC (Fig. 6A,C; n=7), until heterologous synapsis is completed, then disappear (Fig. 6A,C). RPA foci are not associated with the unpaired axes of the 13^1 loop (Fig. 6B,D). However, after synaptic adjustment, RPA foci do appear along the heterologous synapsed regions (Fig. 6B,D; n=10). The RPA signal between the homologous loops, of the 13^1 and 1^{13} translocation chromosomes, which is suggestive of attempted interhomolog interactions (Plug et al., 1997), remains during the process of synaptic adjustment (Fig. 6B,D).

DISCUSSION

The correlation between early MNs and RAD51 foci

MNs, or early meiotic nodules, were originally described as electron-dense nodules associated with asynapsed axial elements (axial cores) or SCs (synapsed axes) during leptonema and zygonema into early pachynema (Albini and Jones, 1987; Anderson and Stack, 1988; Stack and Anderson, 1986). The number of MNs in multicellular eukaryotes is generally several times the observed number of chiasmata, or recombination events reported for the species (Albini and Jones, 1987; Anderson and Stack, 1988). They are associated with axial elements and SCs in euchromatic regions, but are seldom observed along axes associated with heterochromatin (Stack and Anderson, 1986). When homologous axial elements converge and diverge in zygotene nuclei, these nodules are often found at the convergence (Albini and Jones, 1987; Anderson and Stack, 1988). On some, but not all axial elements in *Allium cepa*, MNs are found on both axes at these sites of convergence (Albini and Jones, 1987). In addition to the nodules, but in association with them, electron dense bars (also referred to as fibers) are often found between the axes at these convergent sites (Anderson and Stack, 1988).

Although RAD51 has been localized to early meiotic nodules in plants (Anderson et al., 1997), electron dense nodules on asynapsed axes have not been reported in EM studies of mammals, most likely due to the fact that the silver staining procedure generally used does not stain MNs or RNs. However, the temporal and spatial distribution of RAD51 foci in mouse spermatocytes corresponds in every respect to the above description of MNs. RAD51 foci are found on asynapsed axial elements and briefly on SCs (Ashley et al., 1995; Plug et

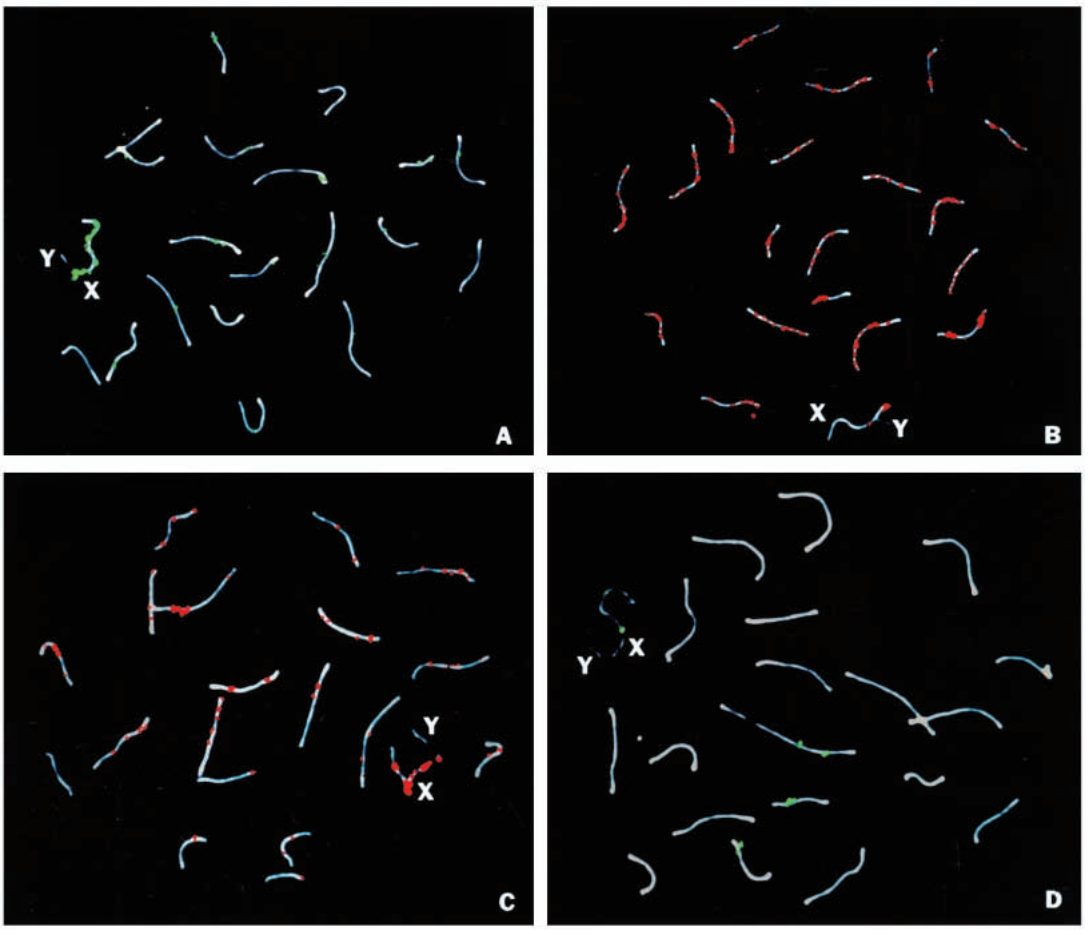

Fig. 4. Temporal distribution of RPA and RAD51 at asynapsed and nonhomologously synapsing regions (COR1: white; RAD51: green; RPA: red). (A) Early-mid pachytene spermatocyte: RAD51 foci are associated with the unsynapsed axial element of the X-chromosome. (B) Early pachytene spermatocyte: RPA foci are present along the SCs, but not the unsynapsed axial element of the X-chromosome. RPA foci appear along the axes of the X-chromosome in mid-late pachytene spermatocytes as the number of RPA autosomal foci is decreasing (C), while RAD51 foci disappear from the X-chromosome during approximately the same time period (D).

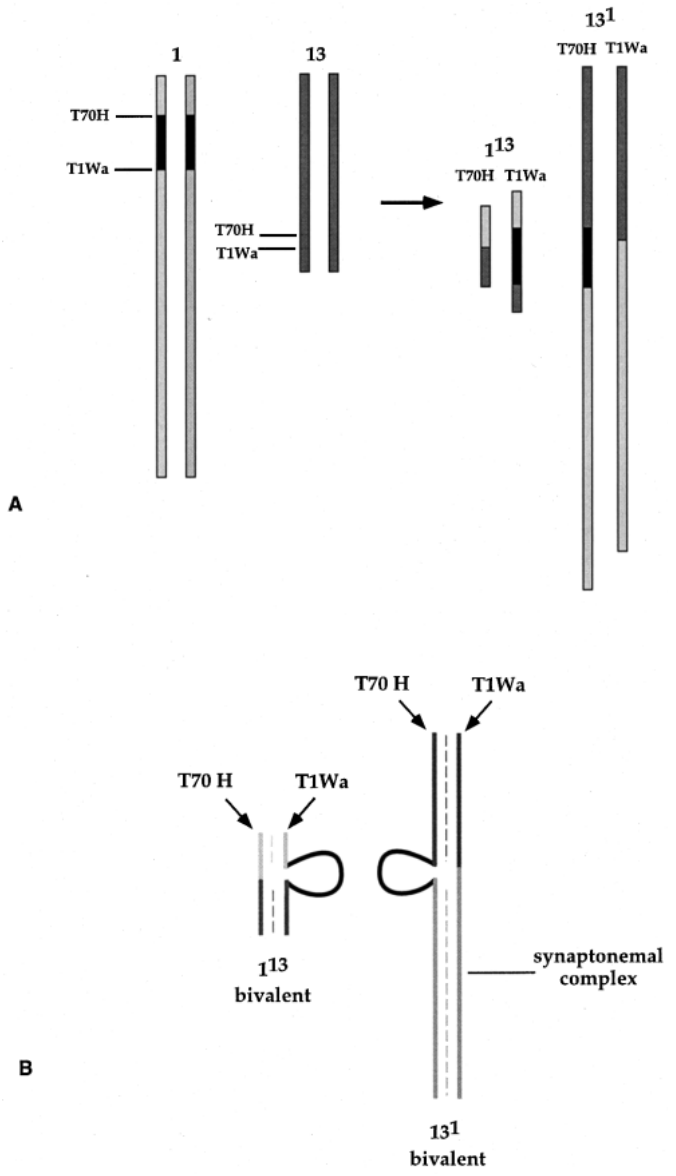

Fig. 5. T(1;13)70H/T(1;13)Wa double heterozygous karyotype. (A) T70H and T1Wa breakpoints on chromosomes 1 and 13. The translocation chromosome that contributed the centromere is indicated first, with the distal portion of the other chromosome indicated by a superscript. (B) A diagram of the homologous synaptic configuration of the 1^{13} and 13^1 heteromorphic bivalents.

al., 1996). In zygotene nuclei RAD51 foci are also found at corresponding sites on converging homologous axes prior to synapsis (Plug et al., 1996). The number of RAD51 foci varies between 90-120 on synapsed axes in early pachytene nuclei (Plug et al., 1996) and is approximately 5-6 times the number of chiasmata (~22) reported for mouse spermatocytes (Polani and Jagiello, 1976). The RAD51 focal pattern in early pachynema appears to correspond to an (euchromatic) R-band pattern and RAD51 foci are absent from the SCs at the centromeric heterochromatic ends of the bivalents (Plug et al., 1996, and present study). The recent report of immunogold clusters of RAD51 antibody signal along asynapsed/newly synapsed axes (Moens et al., 1997) supports the mammalian fluorescence immunolocalization studies (Ashley et al., 1995; Plug et al., 1996). Taken together with the EM localization data from plants, it seems safe to conclude that RAD51 is a component of MNs in mice.

Changes in protein-composition of MNs as homologous chromosomes synapse

Traditional heavy metal stains for electron microscopy allow visualization of proteinaceous structures without identifying individual proteins. Therefore colocalization studies by immunofluorescent antibodies have provided a surprise: a change in protein composition of MNs as homologous chromosomes synapse. Although RAD51 is present on both asynapsed and synapsed axes, RPA appears to be added to these nucleoprotein complexes only as homologs come into close physical proximity. This alteration in protein composition of MNs during synapsis is also seen in the complementary localization of the related protein kinases ATR and ATM along synapsing homologous chromosomes (Keegan et al., 1996). Although this study suggested ATR and ATM were components of ‘early RNs’, here referred to as MNs, formal proof was lacking. If colocalization of a second protein with an identified component of a MN constitutes evidence of the second protein also being a component, colocalization of ATR with RAD51 links these two proteins to the same presynaptic MN nucleoprotein complex. Recently, RPA and ATM have also been shown to colocalize (Plug et al., 1997), and since the current study shows that RPA and RAD51 colocalize on newly synapsed axes, one can infer that RAD51, RPA and ATM are all part of a postsynaptic MN nucleoprotein complex.

Some form of homologous alignment obviously precedes SC formation (see Kleckner and Weiner, 1993). However, the addition of RPA to RAD51 sites occurs at a critical time: as homologous chromosomes synapse. In vitro experiments indicate that without RPA, or some other single-strand binding protein, RAD51 cannot carry out strand exchange (Baumann et al., 1996), an essential step in both reciprocal recombination, and gene conversion (Carpenter, 1987). Given that efficient RAD51 activity requires RPA, the colocalization of RAD51 and RPA during synapsis suggests that an ‘activation’ of RAD51 sites occurs as homologous interactions are being established and implies that prior to this addition, RAD51 may be ‘search inactive’. If this is the case, formation of extensive DSBs prior to this time would appear to be improbable, since breaks without a potential for a homology search would increase the likelihood of genomic damage or massive chromosomal rearrangements.

The switch in colocalization of ATR vs ATM with RAD51 nucleoprotein complexes also coincides with the transition from the postulated ‘search inactive’ to a ‘search active’ form of RAD51. Since ATR and ATM belong to the same family of phosphatidylinositol 3-kinase (PIK)-like kinases which are involved in regulating DNA damage-induced mitotic cell cycle checkpoints (Hoekstra, 1997; Savitsky et al., 1996), it seems likely that the two proteins monitor subsequent steps in the selection and processing of sequences involved in the homology search, synaptic initiation and initiation of meiotic recombination within MNs. Although little is known about the mitotic role of ATR, ATM is clearly involved in damage detection and subsequent cell cycle control. Evidence from both normal vs A-T cell lines (Liu and Weaver, 1993; Lohrer,

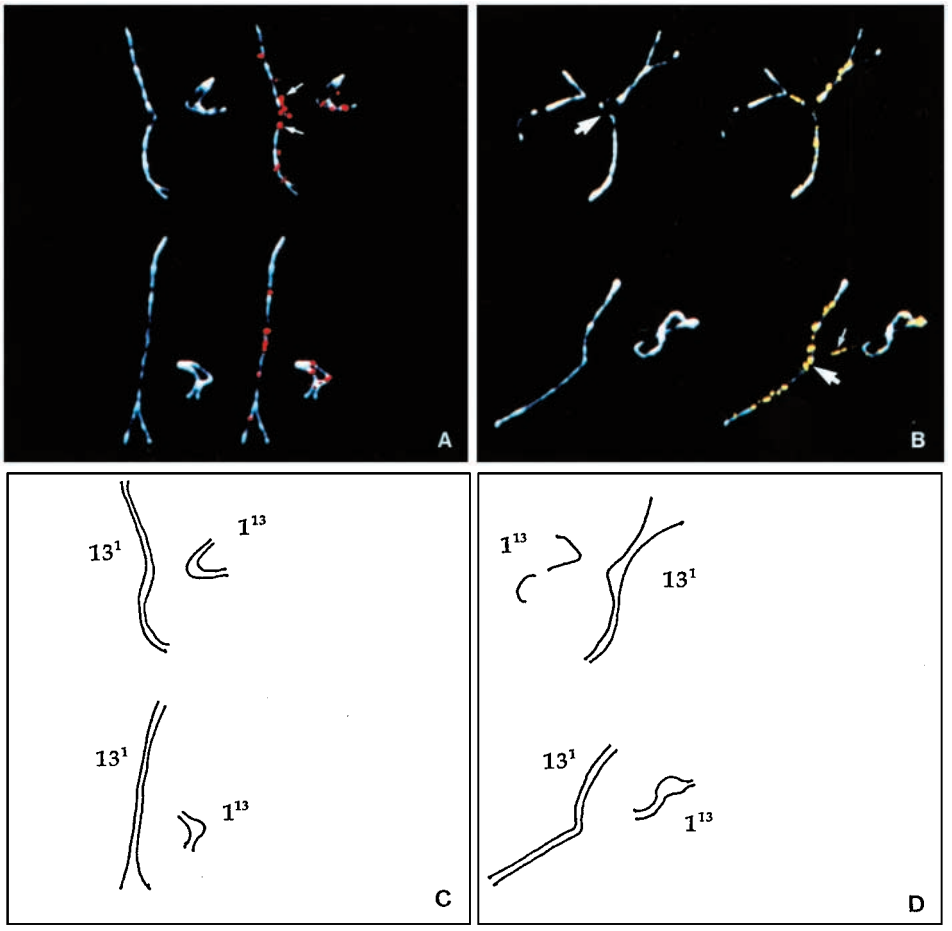

Fig. 6. Temporal distribution of RAD51 and RPA during nonhomologous synapsis (COR1: white; RAD51: red; RPA: yellow). The synaptic configuration of the heteromorphic bivalents as they undergo synaptic adjustment are shown on the left (COR1 only) and the distribution of RAD51 (A), or RPA (B) are shown merged with the COR1 images on the right. The heteromorphic region on the larger 13^1 bivalent (the 'loop' in Fig. 5B) has 'adjusted' (shortened and nonhomologously synapsed), while the heteromorphic region of the small 1^{13} bivalent remains asynapsed. RAD51 (red) foci are present along the asynapsed regions of the 1^{13} (arrows). In addition RAD51 foci are present along the mid-region of the 13^1 heteromorphic region, suggesting that nonhomologous synapsis has only recently occurred. (B) Although RPA (yellow) is not present on the asynapsed region (arrow in upper set of bivalents), RPA foci appear along the nonhomologously synapsed region (arrow, lower set of bivalents). In addition, RPA remains in the region between the two heteromorphic bivalents. (C and D) Interpretative drawings of the synaptic configurations of the synaptically adjusted heteromorphic bivalents in A and B above. Both 13^1 bivalents in A have adjusted (synapsed nonhomologously), while both 1^{13} bivalents are still asynapsed around the region of nonhomology. (B) The upper 13^1 bivalent is still partially asynapsed while the 1^{13} chromosomes remain totally asynapsed (two univalents). In the lower pair the 13^1 bivalent has adjusted (synapsed nonhomologously), while the 1^{13} bivalents are still asynapsed around the region of nonhomology.

1996) and normal mice vs mice homozygous for the targeted disruption of the *Atm* gene (Barlow et al., 1996; Elson et al., 1996; Xu et al., 1996) suggests that ATM is involved in signaling the presence of DNA lesions and prevention of progression of the cell cycle until the damage has been repaired (Beamish et al., 1996; Shiloh, 1995). Recently Plug et al. (1997) have demonstrated that chromosomal fragmentation does not occur randomly along the SCs in *Atm–/–* spermatocytes, but that breaks occur preferentially at RPA sites. Since the current paper shows that RPA is a component of postsynaptic MNs, it appears that breaks, as revealed in *Atm–/–* spermatocytes, occur within the nucleoprotein complexes of *postsynaptic* MNs. These observations emphasize the unique property of meiotic nodules as sites of DNA-protein interactions within a preselected and highly regulated context.

The 'conversion' of a subset of MNs into RNs

Evidence summarized in the Introduction strongly suggests that MLH1 is a component of RNs. Rasmussen and Holm (1980) and Stack et al. (1993) proposed that a subset of early nodules persist and become late nodules. Our results support this supposition and extend it by showing that there is a dynamic change in protein components as recombination intermediates are processed. Although RAD51 is a component of both pre- and postsynaptic MNs, most RAD51 foci disappear by the time the MLH1 foci begin to appear in the transition to mid-pachynema. RPA colocalizes with RAD51 in postsynaptic MNs and remains a component of these structures after RAD51 disappears. Most RPA foci are still present along the SCs when

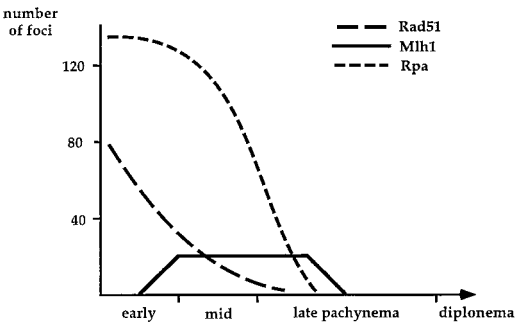

Fig. 7. A schematic representation of the dynamic changes in the number of RAD51, RPA and MLH1 foci associated with the autosomes during pachynema.

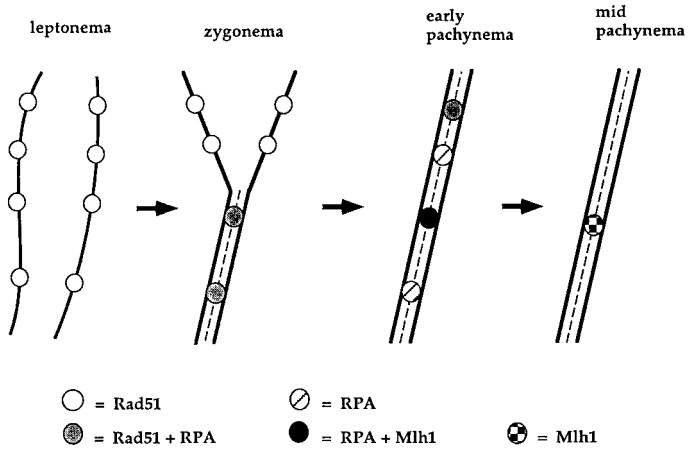

Fig. 8. A schematic representation of the changes in protein composition of meiotic nodules as determined by immunolocalization studies.

MLH1 foci appear and their number stabilizes in mid-pachynema. MLH1 is a component of RNs (Baker et al., 1996). The majority of MLH1 foci colocalize with RPA during this interval. This colocalization suggests that RPA is also a component of RNs as well as MNs. These observations also suggest that any MN has the potential to become an RN and implies that any RAD51-, or RPA-associated sequence within an MN is a candidate sequence for reciprocal recombination. RPA foci then begin to disappear before the number of MLH1 foci also begins to decline during the transition to late pachynema. Fig. 7 illustrates the dynamic changes in the number of RAD51-, RPA-, and MLH1 foci associated with the autosomal SCs during the subsequent substages of pachynema and Fig. 8 diagrams the transition of a subset of MNs to RNs by turnover of RAD51, RPA and MLH1.

Role of RPA during asynapsis and nonhomologous synapsis

RAD51 foci associated with autosomal axes disappear shortly after formation of the SC (synapsis). The X-chromosome has no homolog in spermatocytes and therefore can neither fully synapse, nor undergo reciprocal recombination along most of its length. Yet, RAD51 foci are not only present along its length in late zygonema-early pachynema, but they remain there long after they disappear from the synapsed autosomes. There are no RPA foci along the axial element of the X in early pachynema, but by mid- and mid-late pachynema they appear along the length of X-axis. Both RAD51 and RPA foci then disappear from the X-axis in the transition to late pachynema. A similar process occurs during synaptic adjustment of the unsynapsed axial loop of the 13^1 translocation: as the axes 'adjust' and synapse nonhomologously. RAD51 foci disappear and their disappearance coincides with the appearance of RPA foci appear along the heterosynapsed synapsed region. During both asynapsis and nonhomologous synapsis there appears to be an obligatory processing of RAD51 associated sequences, in the absence of homologous synapsis. The sequential changes in RAD51 and RPA foci that occur under these exceptional circumstances suggest that homologous synapsis is not a prerequisite for the observed processing to occur.

We thank Lorrie Anderson for many stimulating discussions and her comments on the manuscript. We also thank the following for antibodies: Drs Peter Moens and Barbara Spyropoulos for the anti-COR1 antibodies; Charles Radding, Efim Golub, and Gurrucharan Reddy for the affinity-purified RAD51 antiserum; James Ingles for polyclonal antibody against RPA; and Zhen-Quing Pan for the monoclonal antibody against the 70 kDa subunit of RPA. The research was supported by NIH grants GM49779 and GM55300 to T.A. M.F.H. and K.S.K. were supported by ICOS Corporation and A.H.F.M.P. and P. de B. are accredited to the Wageningen Institute of Animal Science.

REFERENCES

Albini, **S. M. and Jones, G. H.** (1987). Synaptonemal complex spreading in Allium cepa and A. fistulosum. I. The initiation and sequence of pairing. *Chromosoma* **95**, 324-338.

Anderson, L. K. and Stack, S. M. (1988). Nodules associated with axial cores and synaptonemal complexes during zygotene in Psilotum nudum. *Chromosoma* **97**, 96-100.

Anderson, L. K., Offenberg, M. M., Verkuijlen, W. H. M. C. and Heyting, C. (1997). RecA-like proteins are components of early meiotic nodules in lily. *Proc. Nat. Acad. Sci. USA* **94**, 6868-6873.

Ashley, T. and Russel, L. B. (1986). A new type of nonhomologous synapsis in T(X;4)1Rl translocation mice. *Cytogen. Cell Genet* **43**, 194-200.

Ashley, T. (1988). G-band position effects on meiotic synapsis and crossing over. *Genetics* **118**, 307-317.

Ashley, T., Plug, A. W., Xu, J., Solari, A. J., Reddy, G., Golub, E. I. and Ward, D. C. (1995). Dynamic changes in Rad51 distribution on chromatin during meiosis in male and female vertebrates. *Chromosoma* **104**, 19-28.

Ashley, T. and Plug, A. W. (1998). Caught in the act: deducing meiotic function from protein immunolocalization. In *Meiosis and Gametogenesis*. *Curr. Topics Dev. Biol.* **37** (ed. M. A. Handel), pp. 201-239. Academic Press, San Diego.

Baker, S. M., Plug, A. W., Prolla, T. A., Bronner, C. E., Harris, A. C., Yao, X., Christie, D.-M., Monell, C., Arnheim, N., Bradley, A., Ashley, T. and Liskay, R. M. (1996). Involvement of mouse MLH1 in DNA mismatch repair and meiotic crossing over. *Nature Genet.* **13**, 336-342.

Barlow, C., Hirotsune, S., Paylor, R., Liyanage, M., Eckhaus, M., Collins, F., Shiloh, Y., Crawley, J. N., Ried, T., Tangle, D. and Wynshaw-Boris, A. (1996) ATM deficient mice: A paradigm of ataxia telangiectasia. *Cell* **86**, 150-171.

Baumann, P., Benson, F. E. and West, S. C. (1996). Human RAD51 protein promotes ATP-dependent homologous pairing and strand transfer reactions in vitro. *Cell* **87**, 757-766.

Beamish, H., Williams, R., Chen, P. and Lavin, M. F. (1996). Defect in multiple cell cycle checkpoints in ataxia-telangiectasia postirradiation. *J. Biol. Chem.* **271**, 20486-20493.

Bishop, D. K. (1994). RecA homologues Dmc1 and Rad51 interact to form multiple nuclear complexes prior to meiotic chromosome synapsis. *Cell* **79**, 1081-1092.

Carpenter, A. T. C. (1975). Electron microscopy of meiosis in Drosophila melanogaster females. II The recombination nodule - a recombination-associated structure in pachytene? *Proc. Nat. Acad. Sci. USA* **72**, 3186-3189.

Carpenter, A. T. C. (1979). Synaptonemal complex and recombination nodules in the wild-type Drosophila melanogaster females. *Genetics* **92**, 511-541.

Carpenter, A. T. C. (1987). Gene conversion, recombination nodules, and the initiation of meiotic synapsis. *BioEssays* **6**, 232-236.

Coverley, D., Kenny, M. K., Munn, M., Rupp, W. D., Lane, D. P. and Wood, R. D. (1991). Requirement for the replication protein SSB in human DNA excision repair. *Nature* **349**, 538-541.

Coverley, D., Kenney, M. K., Lane, D. P. and Wood, R. D. (1992). A role for the human single-stranded DNA binding protein HSSB/RPA in an early stage of nucleotide excision repair. *Nucl. Acids Res.* **20**, 3873-3880.

de Boer, P., Searl, A. G., van der Hoeven, F. A., de Rooij, D. G. and Beechey, C. V. (1986). Male pachytene pairing in single and double translocation heterozygotes and spermatogenic impairment in the mouse. *Chromosoma* **93**, 326-336.

Dobson, M. J., Pearlman, R. E., Karaiskakis, A., Spyropoulos, B. and Moens, P. B. (1994). Synaptonemal complex proteins, epitope mapping and chromosome disjunction. *J. Cell Sci.* **107**, 2749-2760.

Edelmann, W., Cohen, P. E., Kane, M., Lau, K., Morrow, B., Bennett, S., Umar, A., Kunkel, T., Cattoretti, G., Chaganti, R., Pollard, J. W., Kolodner, R. D. and Kucherlapati, R. (1996). Meiotic pachytene arrest in MLH1-deficient mice. *Cell* **85**, 1125-1134.

Elson, A., Wang, Y., Daugherty, C. J., Morton, C. C., Zhou, F., Campos-Torres, J. and Leder, P. (1996). Pleiotrophic defects in ataxia-telangiectasia protein-deficient mice. *Proc. Nat. Acad. Sci.* USA **93**, 13084-13089.

Fairman, M. P. and Stillman, B. (1988). Cellular factors required for multiple stages of SV40 replication in vitro. *EMBO J.* **7**, 1211-1218.

Goetz, P., Chandley, A. C. and Speed, R. M. (1984). Morphological and temporal sequence of meiotic prophase development at puberty in male mouse. *J. Cell Sci.* **65**, 249-263.

Haaf, T., Golub, E. I., Reddy, G., Radding, C. M. and Ward, D. C. (1995). Nuclear foci of mammalian RAD51 recombination protein in somatic cells after DNA damage and its localization in synaptonemal complexes. *Proc. Nat. Acad. Sci. USA* **92**, 2298-2302.

He, Z., Henrickson, L. A., Wold, M. S. and Ingles, C. J. (1995). RPA involvement in the damage-recognition and incision steps of nucleotide excision repair. *Nature* **374**, 566-569.

Heyer, W.-D., Rao, M. R. S., Erdile, L. F., Kelley, T. J. and Kolodner, R. D. (1990). An essential Saccharomyces cerevisiae single-stranded DNA binding protein is homologous to the large subunit of human RP-A. *EMBO J.* **9**, 2321-2329.

Hoekstra, M. F. (1997). Responses to DNA damage and regulation of cell cycle checkpoints by the ATM protein kinase family. *Curr. Opin. Gen. Dev.* **7**, 170-175.

Keegan, K. S., Holtzman, D. A., Plug, A. W., Christenson, E. R., Brainerd, E. E., Flaggs, G., Bentley, N. J., Taylor, E. M., Meyn, M. S., Moss, S. B., Carr, A. M., Ashley, T. and Hoekstra, M. F. (1996). The ATR and ATM protein kinases associate with different sites along meiotically pairing chromosomes. *Genes Dev.* **10**, 2423-2437.

Kenny, M. K., Schlegel, U., Furneaux, H. and Hurwitz, J. (1990). The role of human single-stranded DNA binding protein and its individual subunits in Simian virus 40 DNA replication. *J. Biol. Chem.* **265**, 7693-7700.

Kleckner, N. and Weiner, B. M. (1993). Potential advantages of unstable interactions for pairing of chromosomes in mitotic, somatic and premeiotic cells. *Cold Spring Harbor Symp. Quant. Biol.* **58**, 553-565.

Lammers, J. H. M., Offenberg, H. H., van Aalderen, M., Vink, A. C., Dietrich, A. J. and Heyting, C. (1994). The gene encoding a major component of the lateral element of the synaptonemal complex of the rat is related to X-linked lymphocyte-regulating genes. *Mol. Cell. Biol.* **14**, 1137-1146.

Liu, V. F. and Weaver, D. T. (1993). The ionizing radiation-induced replication protein A phosphorylation response differs between ataxia telangiectasia and normal human cells. *Mol. Cell. Biol.* **13**, 7222-7231.

Lohrer, H. D. (1996). Regulation of the cell cycle following DNA damage in normal and Ataxia telangiectasia cells. *Experientia* **52**, 316-328.

Moens, P. B., Chen, D. J., Shen, Z., Kolas, N., Tarsounas, M., Heng, H. H. Q. and Spyropoulos, B. (1997) Rad51 immunocytology in rat and mouse spermatocytes and oocytes. *Chromosoma* **106**, 207-215.

Moore, S. P., Erdile, L., Kelly, T. and Fishel, R. (1991). The human homologous pairing protein HPP-1 is specifically stimulated by the cognate single-stranded binding protein hRP-A. *Proc. Nat. Acad. Sci. USA* **88**, 9067-9071.

Moses, M. J. (1968). Synaptonemal complex. *Annu. Rev. Genet.* **2**, 363-412.

Moses, M. J. (1980). New cytogenetic studies on mammalian meiosis. In *Animal Models in Human Reproduction* (ed. M. Serio and L. Martini), pp. 169-190. Raven Press, New York.

Moses, M. J. and Poorman, P. A. (1981). Synaptonemal complex analysis of mouse chromosome rearrangements. II. Synaptic adjustment in a tandem duplication. *Chromosoma* **81**, 519-535.

Oakberg, E. F. (1957). Duration of spermatogenesis in the mouse. *Nature* **180**, 1137-1138.

Peters, A. H. F. M., Plug, A. W. and de Boer, P. (1997a). Meiosis in carriers of heteromorphic bivalents: sex differences and implications for male fertility. *Chrom. Res.* **5**, 313-324.

Peters, A. H. F. M., Plug, A. W., van Vugt, M. J. and de Boer, P. (1997b). A drying-down technique for spreading of mammalian meiocytes from the male and female germ line. *Chromosome Res.* **5**, 66-71.

Plug, A. W., Xu, J., Reedy, G., Golub, E. I. and Ashley, T. (1996). Presynaptic association of Rad51 protein with selected sites in meiotic chromatin. *Proc. Nat. Acad. Sci. USA* **93**, 5920-5924.

Plug, A. W., Peters, A. H. F. M., Xu, Y., Keegan, K. S., Hoekstra, M. F., Baltimore, D., de Boer, P. and Ashley, T. (1997). Involvement of ATM and RPA in meiotic chromosome synapsis and recombination. *Nat. Genet.* **17**, 457-461.

Polani, P. E. and Jagiello, G. M. (1976). Chiasmata, meiotic univalents, and age in relation to aneuploid imbalance in mice. *Cytogenet. Cell Genet.* **16**, 505-529.

Rasmussen, S. and Holm, P. B. (1980). Mechanisms of meiosis. *Hereditas* **93**, 187-216.

Ried, T., Baldini, A., Rand, T. and Ward, D. C. (1992). Simultaneous visualization of seven different DNA probes by in situ hybridization using combinatorial fluorescence and digital imaging microscopy. *Proc. Nat. Acad. Sci. USA* **89,** 1388-1392.

Rockmill, B., Sym, M., Scherthan, H. and Roeder, G. S. (1995). Roles for two RecA homologs in promoting meiotic chromosome synapsis. *Genes Dev.* **9**, 2684-2695.

Savitsky, K., Bar-Shira, A., Gilad, S., Rotman, G., Ziv, Y., Vanagaite, L., Tagle, D. A., Smith, S., Uziel, T., Sfez, S. et al. (1996). A single ataxia telangiectasia gene with a product similar to PI-3 kinase. *Science* **268**, 1749-1753.

Shiloh, Y. (1995). Ataxia-telangiectasia: Closer to unraveling the mystery. *Eur. J. Hum. Genet.* **3**, 116-138.

Stack, S. and Anderson, L. (1986). Two-dimensional spreads of synaptonemal complexes from Solanaceous plants II. Synapsis in Lycopersicon esculentum (tomato). *Am. J. Bot.* **73**, 264-281.

Stack, S., Sherman, J., Anderson, L. and Herickhoff, L. (1993). Meiotic nodules in vascular plants. In *Chromosomes Today*, vol. 11 (ed. A. Summer and A. Chandley), pp. 301-311. Chapman & Hall, London.

Sung, P. (1994). Catalysis of ATP-dependent homologous DNA pairing and strand exchange by yeast RAD51 protein. *Science* **265**, 1241-1243.

Terasawa, M., Shinohara, A., Hotta, Y., Ogawa, H. and Ogawa, T. (1995). Localization of RecA-like recombination proteins on chromosomes of lily at various meiotic stages. *Genes Dev.* **9**, 925-934.

Weith, A. and Traut, W. (1980). Synaptonemal complexes with associated chromatin in a moth, Ephestia kuehniella Z. *Chromosoma* **78**, 275-291.

Wettstein, D. v., Rasmussen, S. W. and Holm, P. B. (1984). The synaptonemal complex in genetic segregation. *Annu. Rev. Genet.* **18**, 331-413.

Wobbe, C. R. L., Weissbach, L., Borowiec, J. A., Dean, F. B., Murakami, Y., Bullock, P. and Hurwich, J. (1987). Replication of SV40 origin containing DNA in vitro with purified proteins. *Proc. Nat. Acad. Sci. USA* **84**, 1834-1838.

Wold, M. S. and Kelly, T. (1988). Purification and characterization of replication protein A, a cellular protein required for in vitro replication of simian virus 40 DNA. *Proc. Nat. Acad. Sci. USA* **85**, 2523-2527.

Xu, Y., Ashley, T., Brainerd, E. E., Bronson, R. T., Meyn, M. S. and Baltimore, D. (1996). Targeted disruption of ATM leads to growth retardation, chromosomal fragmentation during meiosis, immune defects, and thymic lymphoma. *Genes Dev.* **10**, 2411-2422.